



Insights into the pore structure characteristics of the Lower Silurian Longmaxi Formation shale in the Jiaoshiba area, Southern Sichuan Basin, China

Jian Xiong^{1,2} · Yukang Li² · Shangwen Zhou³ · Xiangjun Liu² · Hui Han² · Lixi Liang² · Jun Zhao²

Received: 13 October 2021 / Accepted: 9 March 2022 / Published online: 31 March 2022
© The Author(s) 2022

Abstract

In this paper, the pore structure characteristics of shales and its controlling factors were analyzed by means of total organic carbon (TOC) analysis, X-ray diffraction (XRD) analysis, field emission scanning electron microscopy (FE-SEM) and low-pressure N₂ adsorption (LPNA) analysis. Based on the grey relational analysis, the controlling factors of pore structure parameters were discussed. The results showed that the TOC contents range from 2.98 to 4.97%, the main minerals of shales are quartz and clay minerals with an average of 41.62 and 30.98%, respectively. The organic matter pores, the interparticle pores, the intraparticle pores, and the micro-fractures are the main pore types determined by the FE-SEM observation. The pore volume of shales is between 0.0637 and 0.1053 cm³/g, the specific surface area ranges from 16.44 to 37.61 m²/g, the average pore size is between 11.20 and 15.50 nm. The organic matter and the quartz have a positive influence on the specific surface area and total pore volume, whereas the clay minerals have a negative impact. The shales have a wide range of pore size, and the mesopores and macropores are the dominant contributor to the total pore volume while the mesoporous contribute the main specific surface area. The TOC contents and quartz contents have the most significant effect on the total pore volume and specific surface area, and the average pore size is mainly controlled by the quartz contents.

Keywords Longmaxi formation · Shale · Pore structure characteristic · Controlling factor · Grey relational analysis

Introduction

Shale gas is an unconventional natural gas occurring in reservoir rocks dominated by organic-rich shales, which exists in the form of free state, adsorbed state and dissolved state and is a kind of clean and effective energy resources. Shale gas has become the most important energy supply with the increasing shortage of conventional oil and gas resources all over the world (Jarvie et al. 2007; Clarkson et al. 2012; Curtis et al. 2002; Loucks et al. 2009; Jia et al. 2017). In 2015,

the Energy Information Administration reported that the global shale gas reservoirs are estimated to be approximately $214.6 \times 10^{12} \text{ m}^3$ and $31.6 \times 10^{12} \text{ m}^3$ in China, accounting for 14.73% of the global total, indicating that China possesses a significant exploration and development potential in the field of shale gas (EIA 2015). At present, in China, numerous shale gas reservoirs have been discovered in Sichuan Basin, Ordos Basin, Bohai Bay Basin, Songliao Basin and Tarim Basin, etc. (Zou et al. 2010, 2018; Guo et al. 2020a, b; Ding et al. 2013; Gao et al. 2018), and new theories of exploration and development have been applied, the production of the shale gas in China continues to rise, with a production of about $15.4 \times 10^9 \text{ m}^3$ in 2019 (Zhen et al. 2020; Fan et al. 2020). Among many basins where a large number of shale gas reservoirs have been found, major breakthroughs of shale gas exploration and development have been made in the Sichuan Basin, and the commercial exploitation of shale gas has been realized for the first time in the Jiaoshiba area in the Sichuan Basin. (Liang et al. 2015; Ma, 2019; Guo et al. 2020a, b).

✉ Jian Xiong
361184163@qq.com

¹ Shale Gas Evaluation and Exploitation Key Laboratory of Sichuan Province, Chengdu 610091, China
² State Key Laboratory of Oil and Gas Reservoir Geology and Exploitation, Southwest Petroleum University, Chengdu 610500, China
³ PetroChina Research Institute of Petroleum Exploration & Development-Langfang, Langfang 065007, China

The shales generally have the characteristics of various mineral composition, diverse pore morphology and wide pore size distribution, indicating that shales have strong heterogeneity. The existing gas occurs commonly with adsorbed and free gas state in the pore spaces of shales (Jarvie et al. 2002; Ross et al. 2009). Previous studies indicated that the pore structure of shales is an important factor, affecting the occurrence state of shale gas (Hu et al. 2017; Wei et al. 2018). Therefore, the research on the pore structure characteristics of shales is of great significance for exploration and development of shale gas. The pore structure refers to the pore type, the pore morphology and the range of pore size distribution (Fu et al. 2015; Yan et al. 2018). Among them, it is very important to understand the pore size distribution and the parameters affecting the pore structure of rocks. And the pore structure is controlled by geological factors such as mineral compositions and the total organic carbon (TOC). Taking it as a research direction, most of scholars have used the least square method to investigate the relationships among pore structure parameters, TOC, mineral compositions (Liu et al. 2015; Zhang et al. 2019; Wang et al. 2019). These studies have suggested the pore structure parameters of rocks are related to many factors, such as TOC, quartz, clay minerals, etc. However, there are relatively few reports on the analysis of main controlling factors of the pore structure parameters of shales. So, it is necessary to introduce some mathematical methods to study the main controlling factors of the pore structure parameters. The grey relational analysis is a method to provide the best possible solution for multiphase problems and demonstrate the inner relationships without large sample data (Pandya et al. 2020; Jaiprakash et al. 2020). In some parameter correlation studies, the grey relational analysis had been adopted by some scholars to investigate (Chen et al. 2009; Mondal et al. 2013; Wen et al. 2022). These studies have shown that the grey relational analysis can provide quantitative control factors as a mathematical method. Therefore, it is appropriate to using the grey relational analysis to quantitatively evaluate the influences of TOC and mineral compositions on the pore structure characteristics of the shales from the Lower Silurian Longmaxi Formation.

The goals of this paper are to investigate the pore structure and its controlling factors of shales from the Lower Silurian Longmaxi Formation in the Jiaoshiba area of Southern Sichuan Basin in China using X-ray diffraction (XRD) analysis, total organic carbon (TOC) analysis, field emission scanning electron microscopy (FE-SEM) and low-pressure N_2 adsorption (LPNA) analysis. The relationships among the pore volume, the specific surface area and the average pore size were studied. Meanwhile, the pore size distributions of shales were studied by using the Barret-Joyner-Halenda (BJH) method and the LPNA data. Finally, the controlling

factors of pore structure parameters of shales were studied by using the grey relational analysis.

Samples and methods

Data

In order to ensure that the shale core samples can accurately reflect the shale characteristics in the study area, a total of 34 shale samples were collected from some wells (with depth of 2800–3200 m) in the Lower Silurian Longmaxi Formation in the Sichuan Basin, China. The Sichuan basin can be divided into six tectonic zones, has undergone many times of tectonic movements. In the basin, the marine facies shale strata of the Upper Ordovician Wufeng Formation and the Lower Silurian Longmaxi Formation are widely distributed. The Lower Silurian Longmaxi Formation shale with rich organic matter and silicon contents deposited in deep-water shelves. (Zhao et al. 2017; Guo et al. 2020a, b). The lithology of the Longmaxi Formation shale is mainly composed of the black shale, gray-black shale and silty mudstone (Chen et al. 2011; Bai et al. 2013). The experimental shale samples were divided indiscriminately into two batches. Total organic carbon (TOC) and X-ray diffraction (XRD) analysis were performed on 34 samples in the first batch, and 20 shale samples were selected for low-pressure nitrogen adsorption analysis in the second batch.

Experimental methods

Thirty-four shale samples were crushed into powder less than 100 mesh and 100 mesh powder following the experimental needs. Prior to the TOC analysis, the powder less than 100 mesh treated with hydrochloric acid to remove carbonate content, then TOC tests were performed using a LECO CS230 carbon/sulfur analyzer. The remaining 100 mesh powder was analyzed with an X' Pert PRO instrument for XRD according the Chinese National Standards GB/T19145-2003 and GB/T18602-2001.

Seven shale samples were cut into $10 \times 10 \times 3$ mm thin slices for FE-SEM analysis. Before the FE-SEM observation, the shale samples were polished by argon ion with the LEICA EM TIC 3X tri-ion sections polisher. Then the shale samples were coated with gold to increase the conductivity of the surface. Subsequently, the samples were placed in the sample chamber of the field emission environment scanning electron microscope and vacuumed until the vacuum of the sample chamber reached the experimental requirements. Finally, the FE-SEM observation was analyzed by the FEI Quanta 650 FEG. All of the FE-SEM images were obtained for analysis of pore types and morphology.

Twenty shale samples were crushed to grains of 60–80 mesh size for low pressure nitrogen adsorption experiments by using the NOVA200e automatic specific surface and porosity analyzer. The standard of experiment following Chinese National Standard GB/T19587-2004 and GB/T21650.2–2008. Before the experiments, the grains need to out-gassed at 378 K for 24 h. During the experiment, the N₂ adsorption/desorption isotherms of shale samples were measured at relative pressure ranging from 0.010–0.995 at 77 K.

Grey relational analysis

In this paper, to explore the relationships among organic matter content and mineral composition, investigate the main factors affecting the pore structure parameters, the grey relational analysis was used, which is commonly used to determine the interrelationships among the multiple parameters. The grey relational analysis has advantages in solving interrelationships and determining the main controlling factors compared with the least square method.

Basing on the grey relational analysis theory, the pore structure parameters are taken as the reference sequence expressed by Eq. (1), and the TOC contents, the quartz contents, the feldspar contents, the carbonate minerals contents and the clay minerals contents are taken as the factor sequence expressed by Eq. (2).

$$X_0 = \{X_0(k) | k = 1, 2, \dots, n\} \quad (1)$$

$$X_i = \{X_i(k) | k = 1, 2, \dots, n\} (i = 1, 2, \dots, m) \quad (2)$$

where X_i is the influencing factor, n is the sampling points, m is the number of influencing factors.

As the range and units of each data is different, the data would be normalized between 0 and 1 by Eq. (3) and Eq. (4) respectively. When there is a positive correlation between the pore structure parameters and TOC contents, mineral compositions contents, it is normalized by Eq. (3), else, Eq. (4).

$$X'_{ik} = \frac{X_{ik} - X_{i\min}}{X_{i\max} - X_{i\min}} \quad (3)$$

$$X'_{ik} = \frac{X_{i\max} - X_{ik}}{X_{i\max} - X_{i\min}} \quad (4)$$

The grey relational coefficient is computed from the normalized data by Eq. (5).

$$\xi_i(k) = \frac{\min_i \min_k \Delta_i(k) + \rho \max_i \max_k \Delta_i(k)}{\Delta_i(k) + \rho \max_i \max_k \Delta_i(k)} \quad (5)$$

where ρ is distinguishing coefficient, dimensionless ($0 \leq \rho \leq 1$); $\Delta_i(k) = |X_0(k) - X_i(k)|$ is the absolute difference between X_0 and X_i at the point k .

$$\gamma_i = \frac{1}{n} \sum_{k=1}^n \xi_i(k) \quad (6)$$

Due to the numerous numbers of relational coefficients, leading to the dispersed information; the grey relational grade is calculated by averaging the grey relational coefficient using Eq. (6).

Results

TOC and mineralogical compositions

The results of shale samples' TOC and XRD analysis are presented in Fig. 1. As shown in Fig. 1, the TOC contents range from 2.08 to 4.97%, with an average of 3.46%, suggesting that the shales from the Longmaxi Formation in the Jiaoshiba region are rich in the organic matter. Meanwhile, we can observe that there is a wide distribution in mineralogical compositions, indicating that the mineralogical compositions in shales is complex. In addition, shale samples are mainly composed of the quartz and the clay minerals, followed by the carbonates and the feldspars. The brittle mineral contents are between 46.46 and 64.32%, with an average of 54.64%, whereas the clay minerals contents range from 21.45 to 39.08%, with an average of 30.07%, showing that the contents of brittle minerals in shales is higher, but the contents of clay minerals in shales is relatively lower. The main clay minerals are the illite, ranging from 14.82 to 29.27%, with a mean of 22.15%. The pyrite contents are ranged from 2.68 to 5.00%, with an average of 3.61%. Above findings are consistent with the previous studies on shales from the Longmaxi Formation in the Sichuan Basin of China (Xiong et al. 2015; Ji et al. 2020).

Pore morphology

As shown in Fig. 2, the shale samples develop various pore types and the pore size distribute in a wide range from nano-scale to micro-scale. In this work, pore types of the shale samples are categorized into the organic matter (OM) pores and inorganic pores including; interparticle (Inter), intraparticle (Intra), and micro-fractures.

Previous researches (Hu et al. 2017; Liu et al. 2020) have shown that a certain level of thermal maturation is necessary condition for the development of OM pores, which means that the development of OM pores is closely related to the thermal evolution and hydrocarbon generation process. OM pores are distributed widely within organic matters in the

Fig. 1 XRD analysis results for the Longmaxi Formation shales

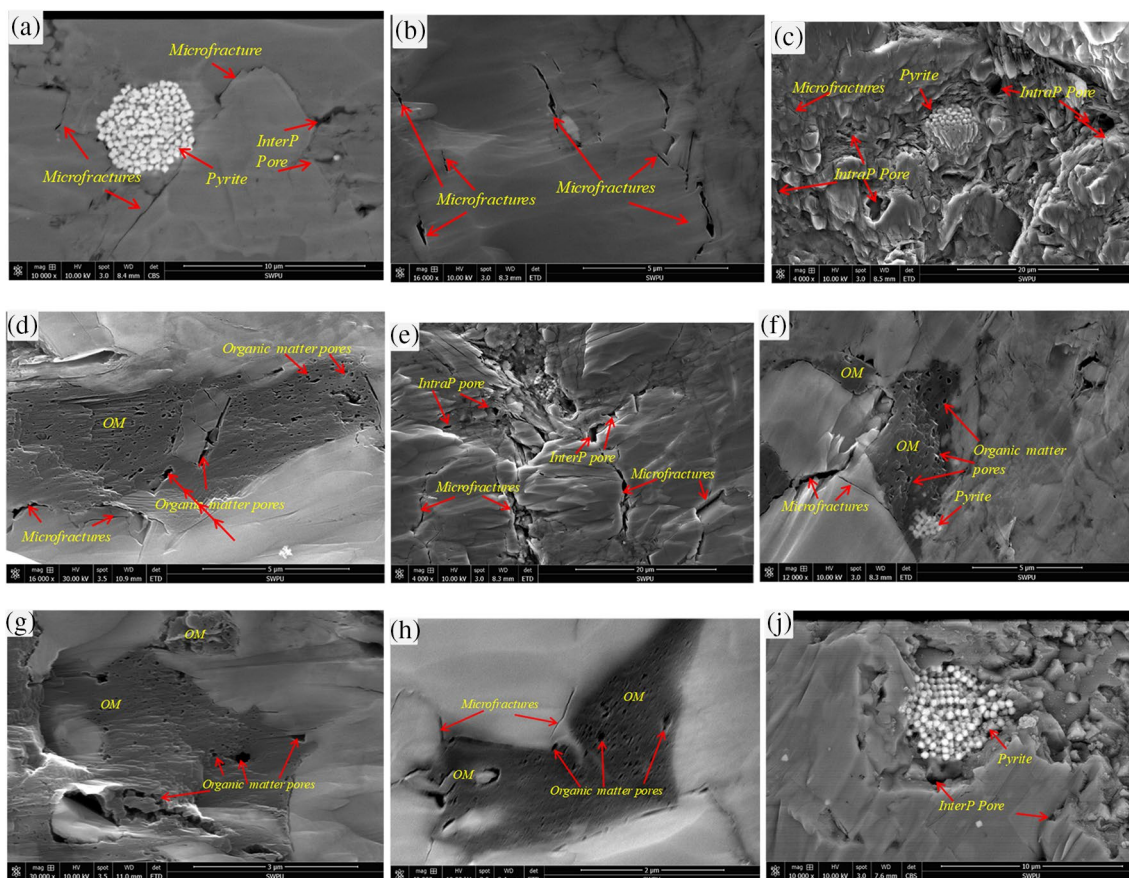
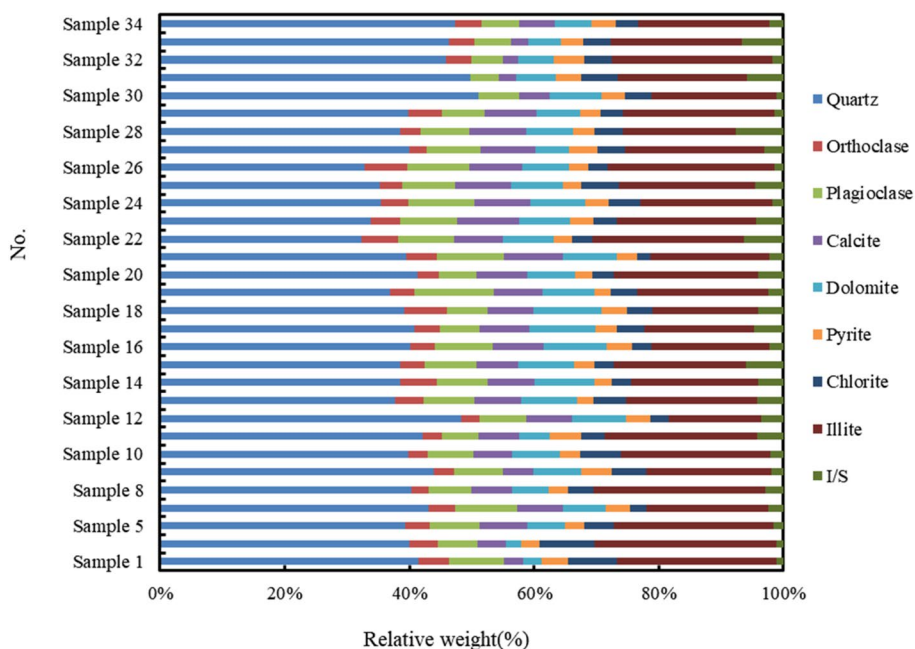


Fig. 2 FE-SEM images of different pore types observed in shale samples. **a** Microfractures, pyrite and interparticle (interP) pores at the depth of 2804 m; **b** microfractures at the depth of 2820 m; **c** microfractures, pyrite and intraparticle (intraP) pores at the depth of 2832 m; **d** organic matter (OM) pores and microfractures at the depth

of 2836 m; **e** intraP pore, interP pores and microfractures at the depth of 2915 m; **f** OM pores and microfractures at the depth of 2953 m; **g** OM pores at the depth of 2981 m; **h** microfractures and OM pores at the depth of 3002 m; **j** interP pores at the depth of 3012 m

study area (Fig. 2d, Fig. 2f, Fig. 2g, Fig. 2h), which are mainly spherical shaped. Meanwhile, OM pores have a huge specific surface area, it means that there are a large number of gas adsorption sites in the pore structure, which is conducive for adsorption and storage of shale gas.

The intergranular pores, developed between mineral grains, are mainly influenced by the degree of compaction, cementation, and overburden pressure. As shown in Fig. 2a, Fig. 2e and Fig. 2j, the intergranular pores are mainly in triangles, polygons, and irregular slits form. These pores are randomly distributed in shale samples. In addition, the intergranular pores commonly have well connectivity, which can provide an effective seepage channel for shale gas. As a result, the development of intergranular pores is conducive to the storage and migration of shale gas. Besides intergranular pores, the intraparticle pores are observed in Fig. 2e and Fig. 2f. The intraparticle pores are spaces developed inside mineral particles such as feldspars and calcites. The morphology of these pores is irregular, and they have poor connectivity. As shown in Fig. 2, compared with interparticle pores the intraparticle pores are not well developed.

In the development of shale gas, the existence of microfractures is very important, which can provide necessary seepage channel and greatly improve the seepage ability of shale gas. Development of microfractures is mainly controlled by tectonic movement, mineral composition, abundance of organic matter, pressure distribution and sedimentary microfacies, etc. (Dong et al. 2018) Image observations suggest that the microfractures in the study area are mainly occupied by tectonic microfractures, and the width ranges from dozens of nanometers to several microns. In addition, the microfractures are developed at the edges of organic matter and other minerals (Fig. 2d, Fig. 2f, Fig. 2g, Fig. 2h). The

kind of microfractures is formed due to the dehydration and shrinkage of the organic matter in the process of organic evolution.

N₂ adsorption–desorption isotherm

Figure 3 (V is the adsorption capacity and P/P_0 is the relative pressure) represents LPNA analysis results in some samples. According to this figure, the desorption branch on the image does not lag, so there is no hysteresis loop, suggesting that shale samples have a closed pore structure. According to the classification types proposed by the International Union of Pure and Applied Chemistry (IUPAC) (Sing et al. 1985), the pore shapes represented by these four classifications are cylindrical holes, ink bottle holes, wedge holes (open at one or both ends) and crack holes. The N₂ adsorption–desorption isotherms of shale samples are similar to H3-type, and have H4-type characteristics, indicating that the shale samples mainly contain wedge holes and cracked holes, and have irregular pore structure characteristics.

Pore size distributions

The plots of $dS/d(\log D)$ vs D (S is the specific surface area and D is the pore size) or $dV/d(\log D)$ vs D (V is the pore volume) can be adopted to present the pore size distribution (Tian et al. 2013; Xiong et al. 2015). According to the results of LPNA experiments, the distribution of the specific surface area or pore volume of some shale samples calculated based on the BJH method are presented in Fig. 4. From Fig. 4, we can note that the distribution of the specific surface area or pore volume among each sample from the Longmaxi Formation have different

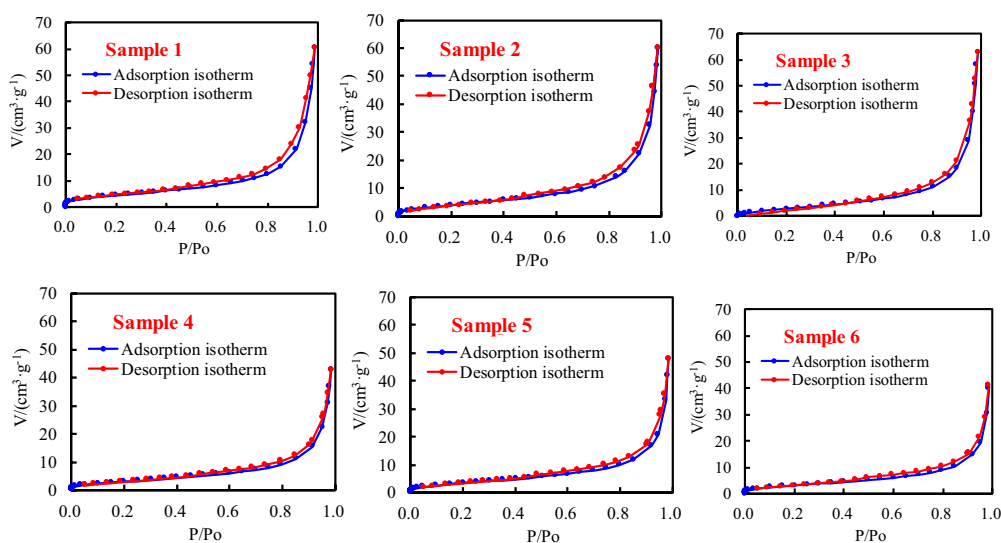


Fig. 3 Low-pressure N₂ adsorption–desorption isotherms of some shale samples

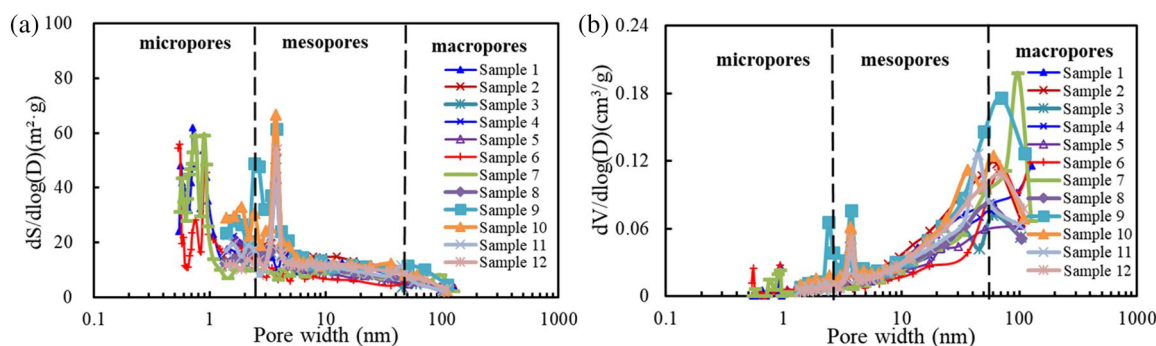


Fig. 4 Specific surface area distribution **a** and pore volume distribution **b** with pore size reconstructed from the isotherms of some shale samples using the BJH method

shapes, and much broader pore size distribution. According to classification type of the pore size presented by the IUPAC (Sing et al. 1985), the pore size was divided into the micropores (< 2 nm), the mesoporous (2–50 nm), and macropores (> 50 nm). The histogram of pore volume and specific surface area of each pore size section of shale samples from Longmaxi Formation are shown in Fig. 5. From Fig. 5(a), we observe that the pore volume of shale samples is mainly composed of mesoporous and macropores, the average pore volume of mesoporous is 65.42%, and the average pore volume of macropores is 31.51%, they account for about 97% of the total pore volume. For the specific surface area, the contribution of mesopores is large (as shown in Fig. 5(b)), which accounting for 66.56–82.79%, with an average of 74.08%, whereas the average contribution of the micropore and macropore to the specific surface area are 17.77 and 8.15%, respectively. The result show that the mesoporous and macropores of shales from the Longmaxi Formation provide the main total pore volume, and the mesopores contribute the main specific surface area.

Pore structure parameters

On the basis of LPNA analysis results, the specific surface area calculated using the BET model, and the N_2 adsorption volume at p/p_0 about 0.98 can be used to estimate pore volume. The pore structure parameters of shale samples are presented in Table 1. As it can be seen from this table, the pore volume ranges from 0.06370 to 0.10532 cm^3/g , with an average of 0.08143 cm^3/g . The specific surface area ranges from 16.44 to 37.61 m^2/g , with an average of 25.87 m^2/g . The average pore size ranges from 11.20 to 15.50 nm, with an average of 12.78 nm, which is classified as mesopore according to the IUPAC classification.

Discussion

Relationship pore structure parameters and TOC, mineral compositions

As shown in Fig. 6, the pore volume and specific surface area of shale samples are positively correlated, and the

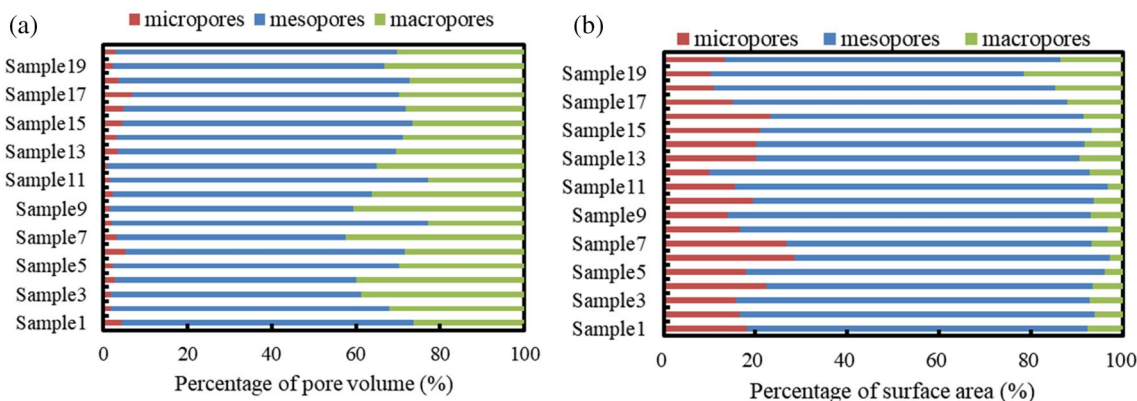


Fig. 5 Percentages of the total pore volume **a** and specific surface area **b** under the IUPAC classification

Table 1 Specific surface area, pore volume and average pore size of shale samples

Sample no	Depth (m)	Pore volume (cm ³ /g)	Specific surface area (m ² /g)	Average pore size (nm)
1	2804	0.07160	20.94	13.68
2	2812	0.07138	21.31	13.40
3	2820	0.09324	31.13	11.98
4	2832	0.06614	19.52	13.56
5	2836	0.09717	31.08	12.50
6	2837	0.08181	27.21	12.02
7	2915	0.07764	23.73	13.08
8	2953	0.06932	21.03	13.18
9	2981	0.06370	16.44	15.50
10	3002	0.07365	22.66	13.00
11	3012	0.10532	37.61	11.20
12	3039	0.09538	32.19	11.85
13	3045	0.09177	29.33	12.52
14	3062	0.07333	22.16	13.24
15	3071	0.09033	29.73	12.15
16	3080	0.07161	21.30	13.45
17	3093	0.08289	27.88	11.89
18	3125	0.09317	31.45	11.85
19	3131	0.09544	32.03	11.92
20	3134	0.06372	18.60	13.70

correlation coefficient is 0.9795, while the average pore size is negatively correlated with pore volume and specific surface area, and the correlation coefficients are 0.7412 and 0.8393 respectively, indicating that the shales with smaller pore is conducive to the storage of shale gas (Bustin et al. 2008; Ross et al. 2009; Xiong et al. 2015; Liu et al. 2015; 2020).

The relationships among the TOC contents, the clay mineral contents, the quartz contents and the total pore volume, the specific surface area, the average pore size (as shown in Figs. 7, 8 and 9) are established to explore the influencing

factors of the pore development of shales from Longmaxi Formation in the study block. From Figs. 7–9, the TOC, clay mineral contents and the quartz contents are the main influencing factors of the total pore volume, the specific surface area, and the average pore size of shales.

From Fig. 7, we observe that the total pore volume of shales is positively correlated with the TOC (Fig. 7a) and the quartz contents (Fig. 7(b)), with correlation coefficients of 0.8060 and 0.7470, respectively. The total pore volume of shales is negatively correlated with the clay mineral contents (Fig. 7c), with correlation coefficient of 0.6298. Meanwhile, from Fig. 8, we observe that the specific surface area is positively correlated with the TOC (Fig. 8a) and the quartz contents (Fig. 8b), with correlation coefficients of 0.8143 and 0.7560, respectively. There is a negatively relationship between the specific surface area and the clay mineral contents (Fig. 8c), with correlation coefficient of 0.6117. The shale samples from Longmaxi Formation with more the TOC contents have larger total pore volume and specific surface area. And with the increase of the quartz contents, the total pore volume and the specific surface area of shales can increase. This may be because that the quartz originates from the biogenesis (siliceous organisms). With the increase of the siliceous components in shales, the number of micropores can increase, resulting in the increase of the total pore volume and the specific surface area (Xiong et al. 2015). However, from Fig. 9, the clay mineral contents in shales can enhance the compaction in the diagenetic process, leading to dense mineral arrangement and reducing the total pore volume and specific surface area. This has similarities (the clay minerals had a negative influence on the specific surface area and pore volume, especially the micropore structure parameters.) and difference (the clay-rich rocks have higher porosity and permeability than the biogenic silica-rich shales or the carbonate-rich shales.) with conclusion found by previous scholars (Bustin et al. 2008; Ross et al. 2009; Xiong et al. 2015). In the end, analyzed from horizontal, the

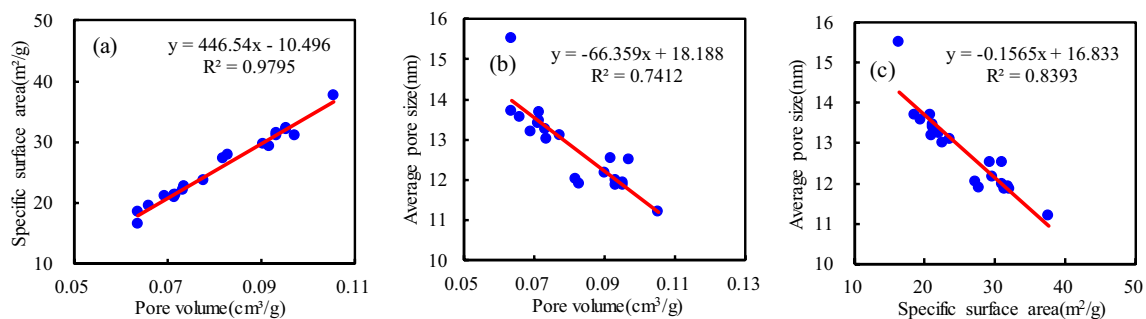


Fig. 6 Relationships between **a** pore volume and specific surface area, **b** average pore size specific surface area and pore volume; **c** average pore size and specific surface area in shale samples

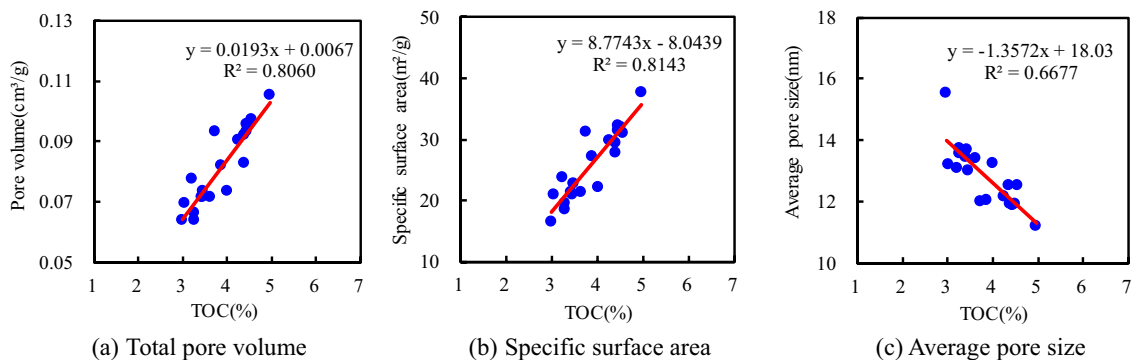


Fig. 7 Relationships between the TOC and **a** total pore volume, **b** specific surface area **c** average pore size

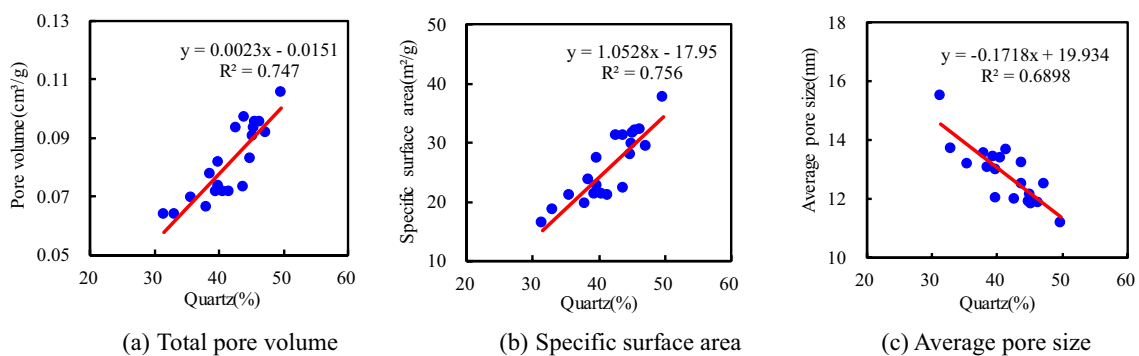


Fig. 8 Relationships between the quartz contents and **a** total pore volume, **b** specific surface area **c** average pore size

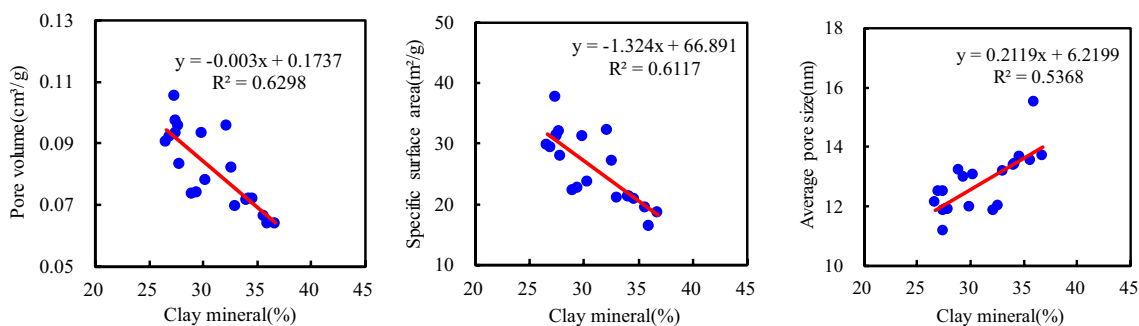


Fig. 9 Relationships between the clay mineral contents and **a** total pore volume, **b** specific surface area **c** average pore size

average pore size is negatively correlated with the total pore volume and the specific surface area according to the result of analysis. This conclusion is in agreement with previous works, such as shales from the Lower Cambrian Niutitang Formation (Yang et al. 2014; Liu et al. 2020), Upper Ordovician Wufeng Formation (Xiong et al. 2015).

The controlling factors on the pore structure characteristics

In this work, we try to introduce the grey correlation analysis method to find the important controlling factors of pore structure characteristics. As shown in Tables 2, 3 and 4,

Table 2 The results of grey relational analysis of the total pore volume

	Sample no	Depth(m)	TOC	Quartz	Feldspars	Carbonates	Clay minerals
Grey relation co-efficient	1	2804	0.91	0.57	0.49	0.41	0.95
	2	2812	0.77	0.60	0.90	0.43	0.86
	3	2820	0.59	0.83	0.82	0.72	0.93
	4	2832	0.84	0.61	0.33	0.70	0.90
	5	2836	0.97	0.79	0.69	0.55	0.81
	6	2837	0.97	0.95	0.60	0.71	0.94
	7	2915	0.69	0.90	0.97	0.58	0.61
	8	2953	0.81	0.84	0.93	0.83	0.67
	9	2981	1.00	1.00	1.00	0.84	0.87
	10	3002	1.00	0.68	0.84	0.71	0.49
	11	3012	1.00	1.00	0.90	0.77	0.86
	12	3039	0.95	0.90	0.81	0.66	0.60
	13	3045	0.94	0.71	0.83	0.77	0.62
	14	3062	0.62	0.51	0.56	0.75	0.47
	15	3071	0.99	0.81	0.93	0.55	0.57
	16	3080	0.94	0.65	0.42	0.72	0.89
	17	3093	0.66	0.63	0.55	0.68	0.53
	18	3125	0.94	0.90	0.85	0.58	0.70
	19	3131	0.99	0.97	0.66	0.63	0.79
	20	3134	0.76	0.84	0.75	0.70	1.00
Grey relation grade			0.87	0.78	0.74	0.66	0.75
rank			1	2	4	5	3

Table 3 The results of grey relational analysis of the specific surface area

	Sample no	Depth(m)	TOC	Quartz	Feldspars	Carbonates	Clay minerals
Grey relation co-efficient	1	2804	0.95	0.56	0.48	0.39	1.00
	2	2812	0.82	0.61	0.98	0.42	0.93
	3	2820	0.57	0.85	0.83	0.72	0.95
	4	2832	1.00	0.67	0.33	0.79	0.93
	5	2836	0.81	0.98	0.81	0.60	0.66
	6	2837	0.87	0.90	0.64	0.61	0.80
	7	2915	0.66	0.91	0.94	0.55	0.59
	8	2953	0.69	0.98	0.78	0.71	0.74
	9	2981	1.00	1.00	1.00	0.83	0.86
	10	3002	0.89	0.72	0.93	0.63	0.50
	11	3012	1.00	1.00	0.89	0.75	0.84
	12	3039	0.99	0.85	0.77	0.63	0.59
	13	3045	0.82	0.62	0.73	0.85	0.54
	14	3062	0.63	0.51	0.56	0.79	0.46
	15	3071	0.96	0.78	0.95	0.53	0.53
	16	3080	0.98	0.67	0.41	0.75	0.96
	17	3093	0.72	0.68	0.58	0.59	0.56
	18	3125	0.94	0.89	0.84	0.55	0.68
	19	3131	0.93	0.91	0.66	0.63	0.73
	20	3134	0.91	0.97	0.89	0.81	0.81
Grey relation grade			0.86	0.80	0.75	0.66	0.73
Rank			1	2	3	5	4

Table 4 The results of grey relational analysis of the average pore size

	Sample no	Depth(m)	TOC	Quartz	Feldspars	Carbonates	Clay minerals
Grey relation co-efficient	1	2804	0.62	0.71	0.54	0.40	0.59
	2	2812	0.65	0.97	0.54	0.48	0.57
	3	2820	0.41	0.60	0.59	0.51	0.67
	4	2832	0.50	0.76	0.35	0.61	0.47
	5	2836	0.77	0.95	0.74	0.51	0.58
	6	2837	0.45	0.46	0.84	0.35	0.43
	7	2915	0.40	0.63	0.55	0.35	0.80
	8	2953	0.37	0.49	0.41	0.38	0.64
	9	2981	1.00	1.00	1.00	0.77	0.81
	10	3002	0.47	0.71	0.54	0.36	0.68
	11	3012	1.00	1.00	0.85	0.68	0.79
	12	3039	0.73	0.90	0.93	0.66	0.43
	13	3045	0.97	0.63	0.80	0.65	0.52
	14	3062	0.97	0.67	0.80	0.68	0.55
	15	3071	0.69	0.92	0.64	0.36	0.58
	16	3080	0.54	0.90	0.45	0.75	0.57
	17	3093	0.69	0.75	0.97	0.33	0.88
	18	3125	0.73	0.77	0.57	0.38	0.82
	19	3131	0.82	0.85	0.49	0.46	0.84
	20	3134	0.52	0.48	0.53	0.58	0.42
Grey relation grade			0.67	0.76	0.66	0.51	0.63
Rank			2	1	3	5	4

the grey correlation coefficient and grey correlation degree of different pore structure parameters including the total pore volume, the specific surface area and the average pore size are presented, respectively. The higher the grey relational grade, the stronger the correlation with pore structure parameters. From Tables 2–4, the order of grey relational grade influencing the total pore volume was determined as the TOC > Quartz > Clay minerals > Feldspars > Carbonates, the order of grey relational grade influencing the specific surface area was determined as the TOC > Quartz > Feldspars > Clay minerals > Carbonates, and the order of grey relational grade influencing the average pore size was determined as the Quartz > TOC > Feldspars > Clay minerals > Carbonates. Therefore, based on the grey relational theory, the TOC contents and the quartz contents have a higher grey correlation in the total pore volume and the specific surface area, indicating that the TOC contents and the quartz contents have an obvious effect on the total pore volume and the specific surface area. And the average pore size is mainly influenced by the quartz contents.

Conclusions

In this study, the pore structure characteristics, and its controlling factors of shale samples from the Lower Silurian Longmaxi Formation in the southern Sichuan Basin of

China were studied by TOC, XRD, FE-SEM, LPNA analysis and grey relational analysis. The major conclusions are as follows:

- (1) The shale samples are rich in organic matter, and the TOC contents are between 2.94 and 4.97% with an average of 3.50%, this formation are mainly composed of quartz (average 40.60%) and clay minerals (average 30.07%). The OM pores, the interparticle pores, the intraparticle pores, and the micro-fractures are the main pore types determined by the FE-SEM observation.
- (2) The pore volume of shale samples is from 0.0637 to 0.1053 cm³/g, the specific surface area ranges from 16.44 to 37.61 m²/g, the average pore size is between 11.20 and 15.50 nm. The TOC and the quartz contents have a positive influence on the specific surface area and total pore volume while the clay minerals contents have a negative impact.
- (3) The TOC contents and quartz contents have the most significant effect on the total pore volume and specific surface area, and the average pore size is mainly controlled by the quartz contents.

Funding This study was funded by the Open Fund of Shale Gas Evaluation and Exploitation Key Laboratory of Sichuan Province (No. YSK2022006), National Natural Science Foundation of China (No.

41602155/41872167), and Young Scientific and Technological Innovation Team of Rock Physics in Unconventional Strata of Southwest Petroleum University (No. 2018CXTD13).

Open Access This article is licensed under a Creative Commons Attribution 4.0 International License, which permits use, sharing, adaptation, distribution and reproduction in any medium or format, as long as you give appropriate credit to the original author(s) and the source, provide a link to the Creative Commons licence, and indicate if changes were made. The images or other third party material in this article are included in the article's Creative Commons licence, unless indicated otherwise in a credit line to the material. If material is not included in the article's Creative Commons licence and your intended use is not permitted by statutory regulation or exceeds the permitted use, you will need to obtain permission directly from the copyright holder. To view a copy of this licence, visit <http://creativecommons.org/licenses/by/4.0/>.

References

- Bai Q, Liu SG, Sun W, Ran B, Luo C, Yang D, Zhang X (2013) Reservoir characteristics of Wufeng Formation Longmaxi Formation in southwest of Sichuan Basin, China. *J Chengdu Univ Technol: Sci Technol Edition* 40(5):521–531
- Bustin RM, Bustin AM, Cui A, Ross D, Pathi VM (2008) Impact of shale properties on pore structure and storage characteristics. In SPE shale gas production conference. OnePetro
- Chen F, Ou T (2009) Gray relation analysis and multilayer functional link network sales forecasting model for perishable food in convenience store. *Expert Syst Appl* 36(3):7054–7063
- Chen S, Zhu Y, Wang H, Liu H, Wei W, Fang J (2011) Shale gas reservoir characterisation: a typical case in the southern Sichuan Basin of China. *Energy* 36(11):6609–6616
- Clarkson CR, Jensen JL, Pedersen PK, Freeman M (2012) Innovative methods for flow-unit and pore-structure analyses in a tight siltstone and shale gas reservoir. *AAPG Bull* 96(2):355–374
- Curtis JB (2002) Fractured shale-gas systems. *AAPG Bull* 86(11):1921–1938
- Ding W, Zhu D, Cai J, Gong M, Chen F (2013) Analysis of the developmental characteristics and major regulating factors of fractures in marine–continental transitional shale-gas reservoirs: a case study of the Carboniferous-Permian strata in the southeastern Ordos Basin, central China. *Mar Pet Geol* 45:121–133
- Dong D, Shi Z, Sun S et al (2018) Factors controlling microfractures in black shale: a case study of Ordovician Wufeng Formation-Silurian Longmaxi Formation in Shuanghe Profile, Changning area, Sichuan Basin. *SW China Petrol Explor Develop* 45(5):818–829
- Energy Information Administration (EIA), 2015 Technically recoverable shale oil and shale gas resources: an assessment of 137 shale formations in 46 countries outside the United States
- Fan C, Li H, Qin Q, He S, Zhong C (2020) Geological conditions and exploration potential of shale gas reservoir in Wufeng and Longmaxi Formation of southeastern Sichuan Basin, China. *J Petrol Sci Eng* 191:107138
- Fu H, Wang X, Zhang L, Gao R, Li Z, Xu T, Zhu X, Xu W, Li Q, Li Q (2015) Investigation of the factors that control the development of pore structure in lacustrine shale: a case study of block X in the Ordos Basin, China. *J Natural Gas Sci Eng* 26:1422–1432
- Gao F, Song Y, Li Z, Xiong F, Chen L, Zhang Y, Liang Z, Zhang X, Chen Z, Joachim M (2018) Lithofacies and reservoir characteristics of the lower cretaceous continental shahezi shale in the changling fault depression of songliao basin, NE China. *Mar Pet Geol* 98:401–421
- Guo X, Hu D, Huang R et al (2020a) Deep and ultra-deep natural gas exploration in the Sichuan Basin: progress and prospect[J]. *Natural Gas Industry B* 7(5):419–432
- Guo X, Li Y, Borjigen T, Wang Q, Yuan T, Shen B, Ma Z, Wei F (2020b) Hydrocarbon generation and storage mechanisms of deep-water shelf shales of Ordovician Wufeng Formation-Silurian Longmaxi Formation in Sichuan Basin China. *Petrol Explor Develop* 47(1):204–213
- Hu H, Hao F, Lin J, Lu Y, Ma Y, Li Q (2017) Organic matter-hosted pore system in the Wufeng-Longmaxi (O3w-S11) shale, Jiaoshiha area, eastern Sichuan Basin, China. *Int J Coal Geol* 173:40–50
- Jaiprakash M, Nagamadhu M, Karthikeyan K, Kumar GM (2020) Effect of drilling parameters on Neem wood veneer epoxy composites using grey relational analysis. *Mater Today: Proc* 24:2163–2173
- Jarvie DM, Hill RJ, Ruble TE, Pollastro RM (2007) Unconventional shale-gas systems: the Mississippian Barnett Shale of north-central Texas as one model for thermogenic shale-gas assessment. *AAPG Bull* 91(4):475–499
- Ji W, Hao F, Song Y, Tian J, Meng M, Huang H (2020) Organic geochemical and mineralogical characterization of the lower Silurian Longmaxi shale in the southeastern Chongqing area of China: implications for organic matter accumulation. *Int J Coal Geol* 220:103412
- Jia C (2017) Breakthrough and significance of unconventional oil and gas to classical petroleum geology theory. *Pet Explor Dev* 44(1):1–10
- Liang L, Xiong J, Liu X (2015) Mineralogical, microstructural and physiochemical characteristics of organic-rich shales in the Sichuan Basin, China. *J Natural Gas Sci Eng* 26:1200–1212
- Liu X, Xiong J, Liang L (2015) Investigation of pore structure and fractal characteristics of organic-rich Yanchang formation shale in central China by nitrogen adsorption/desorption analysis. *J Natural Gas Sci Eng* 22:62–72
- Liu Z, Yan D, Niu X (2020) Insights into pore structure and fractal characteristics of the lower cambrian niutitang formation shale on the Yangtze Platform, South China. *J Earth Sci* 31(1):169–180
- Loucks RG, Reed RM, Ruppel SC, Jarvie DM (2009) Morphology, genesis, and distribution of nanometer-scale pores in siliceous mudstones of the Mississippian Barnett Shale. *J Sediment Res* 79(12):848–861
- Ma X (2019) Enrichment laws and scale effective development of shale gas in the southern Sichuan Basin[J]. *Natural Gas Industry B* 6(3):240–249
- Mondal S, Paul C, Kukreja L, Bandyopadhyay A, Pal P (2013) Application of Taguchi-based gray relational analysis for evaluating the optimal laser cladding parameters for AISI1040 steel plane surface. *Int J Adv Manuf Technol* 66(1–4):91–96
- Pandya VJ, Rathod PP (2020) Optimization of mechanical properties of green composites by gray relational analysis. *Mater Today: Proc* 27:19–22
- Ross DJ, Bustin RM (2009) The importance of shale composition and pore structure upon gas storage potential of shale gas reservoirs. *Mar Pet Geol* 26(6):916–927
- Sing KS (1985) Reporting physisorption data for gas/solid systems with special reference to the determination of surface area and porosity (Recommendations 1984). *Pure Appl Chem* 57(4):603–619
- Tian H, Pan L, Xiao X, Wilkins RW, Meng Z, Huang B (2013) A preliminary study on the pore characterization of Lower Silurian black shales in the Chuandong Thrust Fold Belt, southwestern China using low pressure N₂ adsorption and FE-SEM methods. *Mar Pet Geol* 48:8–19
- Wang Y, Liu L, Zheng S, Luo Z, Sheng Y, Wang X (2019) Full-scale pore structure and its controlling factors of the Wufeng-Longmaxi shale, southern Sichuan Basin, China: Implications for pore

- evolution of highly overmature marine shale. *J Natural Gas Sci Eng* 67:134–146
- Wei Z, Wang Y, Wang G, Sun Z, Xu L (2018) Pore characterization of organic-rich Late Permian Da-long Formation shale in the Sichuan Basin, southwestern China. *Fuel* 211:507–516
- Wen P, Li L, Xue H, Jia Y, Gao L, Li R, Huo L (2022) Comprehensive evaluation method of the poultry house indoor environment based on gray relation analysis and analytic hierarchy process. *Poultry Sci* 101(2):101587
- Xiong J, Liu X, Liang L (2015) Experimental study on the pore structure characteristics of the Upper Ordovician Wufeng Formation shale in the southwest portion of the Sichuan Basin, China. *J Natural Gas Sci Eng* 22:530–539
- Yan J, Zhang S, Wang J, Hu Q, Wang M, Chao J (2018) Applying fractal theory to characterize the pore structure of lacustrine shale from the Zhanhua Depression in Bohai Bay Basin Eastern China. *Energy Fuels* 32(7):7539–7556
- Yang F, Ning Z, Liu H (2014) Fractal characteristics of shales from a shale gas reservoir in the Sichuan Basin, China. *Fuel* 115:378–384
- Zhang J, Li X, Zou X, Zhao G, Zhou B, Li J, Xie Z, Wang F (2019) Characterization of the full-sized pore structure of coal-bearing shales and its effect on shale gas content. *Energy Fuels* 33(3):1969–1982
- Zhao J, Jin Z, Jin Z, Wen X, Geng Y, Yan C, Nie H (2017) Depositional environment of shale in Wufeng and Longmaxi Formations Sichuan Basin. *Petrol Res* 2(3):209–221
- Zou C, Dong D, Wang S, Li J, Li X, Wang Y, Li D, Cheng K (2010) Geological characteristics and resource potential of shale gas in China. *Pet Explor Dev* 37(6):641–653
- Zou YR, Sun JN, Li Z, Xu X, Li M (2018) Evaluating shale oil in the Dongying Depression, Bohai Bay Basin, China, using the over-saturation zone method. *J Petrol Sci Eng* 161:291–301

Publisher's Note Springer Nature remains neutral with regard to jurisdictional claims in published maps and institutional affiliations.